CHARACTERIZATION OF BEHIND-ARMOR DEBRIS PARTICLES FROM TUNGSTEN PENETRATORS

B. Pedersen, S. Bless

Institute for Advanced Technology, 3925 W. Braker Lane, Ste. 400 Austin, TX 78759

Behind-armor debris (BAD) is affected by penetrator parameters: impact velocity and diameter. In [1, 2], we reported on the effects of velocity. In this paper, we will report on the effects of penetrator diameter. Targets were 6061-T6 aluminum, and penetrators were 91% W-Ni-Co alloy. Behind the target there was a witness pack composed of five steel plates of increasing thickness. Velocities were 1.7 to 2.6 km/s. Measurements primarily consisted of witness plate perforation patterns.

It was found that as diameter was increased, there was little change in the number of debris particles generated, as measured by the number of perforations in the first witness plate. However, the penetrating power of the particles strongly increased with rod diameter as seen by the increase in number of holes in witness plates three through five.

INTRODUCTION AND BACKGROUND

Modern military vehicles are damaged and experience loss of function because of behind-armor effects. Either the residual penetrator, eroded particles from the penetrator, or ejected target material strikes the operators or damages vehicle systems. The eroded penetrator particles and the ejected target material are known collectively as behind-armor debris (BAD). The development of electromagnetic guns can result in much higher velocities, albeit with smaller projectiles. Therefore, this study was aimed at determining the effects of velocity and penetrator diameter on the debris.

Several studies have been performed looking at velocity effects on behind-armor debris from tungsten rod penetrators against thick steel targets. In an earlier study [3, 4] conducted at the Institute for Advanced Technology (IAT), tungsten rods with a length-to-diameter ratio (*L*/*D)* of 30 were fired at 450 mm steel targets at 1.75 and 2.55 km/s. The study reported that, as velocity increased, so did the number of penetrations into the witness plate. The debris was also spread more uniformly over a larger angle behind the target at higher velocities. Lynch [5] and Hohler et al. [6], showed similar results with higher velocity yielding more perforating debris particles.

The armor found on many modern military vehicles is made using aluminum alloys. There has been very little work, either theoretical or experimental, to understand behind-armor debris in aluminum targets. This is especially true for the high muzzle velocities electromagnetic guns are capable of firing.

In [1, 2], the BAD from tungsten rods against aluminum targets was studied as a function of target thickness and impact velocity. It was found that as velocity increased, so too did the number of perforating debris particles. The effect of target thickness on the total number of generated debris particles was found to be insignificant.

Low velocity tests were performed by Farrand [7] using L/D 10 tungsten rods at 1.35 km/s against aluminum targets. Rods were fired at three scales (1.0, 1.4, and 1.8) to look at the effect of rod diameter. The results of the study were that the penetration capability of the fragments scaled with the penetrator scale. In other words, as the rod diameter increased, so, too, did the fragment size and thus penetration capability.

The goal of the present study was to experimentally investigate and characterize the behind-armor debris generated by the impact of tungsten heavy alloy (WHA) penetrators against thick aluminum targets. Impact velocity and penetrator diameter were varied to gauge their effect on the behind-armor debris.

EXPERIMENTS

Experiments were conducted using the IAT's 115/38 mm two-stage light-gas gun. The penetrators used in the experiments were made from WHA. The alloy used was 91% W, 7% Ni, 3% Co by volume, supplied by Aerojet Ordnance Tennessee. The penetrators were right-circular cylinders with hemispherical noses. *L*/*D* of 20 was chosen with a length of 127 mm. This length and *L*/*D* defined the rod diameter as 6.35 mm. The larger diameter rod was of 9.53 mm. Since the length was kept constant, the larger rod had an L/D of 13.

Targets were 127 mm diameter 6061-T6 aluminum. For aluminum targets almost all penetrating debris is generated from the tungsten that erodes from the penetrator during penetration. Targets of three nominal thicknesses were considered in this study: 75, 100, and 150 mm. The targets were placed into a 6061-T6 aluminum containment fixture that was designed to reduce the possible effects of free lateral boundaries.

Behind the aluminum target was a behind-armor debris witness pack. This was used to capture the penetration signature of the debris particles and to see how deeply they could penetrate into the plate array. In addition, by counting the number of perforations in the first plate, the number of generated behind-armor debris particles could be determined. This target element was spaced 864 mm behind the target and was composed of five pieces of steel, each separated by a 25.4 mm thick piece of Styrofoam. The plate array was composed of (in order) two plates 0.8 mm thick, two plates 1.6 mm thick, and a final plate 3.2 mm thick. The lateral dimensions of the array were 610 mm.

The final target element was a block of armor steel to stop whatever part of the penetrator made it through both the aluminum target and the behind-armor debris witness pack. This block of steel was made of rolled homogeneous armor (RHA) and was placed 254 mm behind the behind-armor debris witness pack. Figure 1 shows a schematic of the setup.

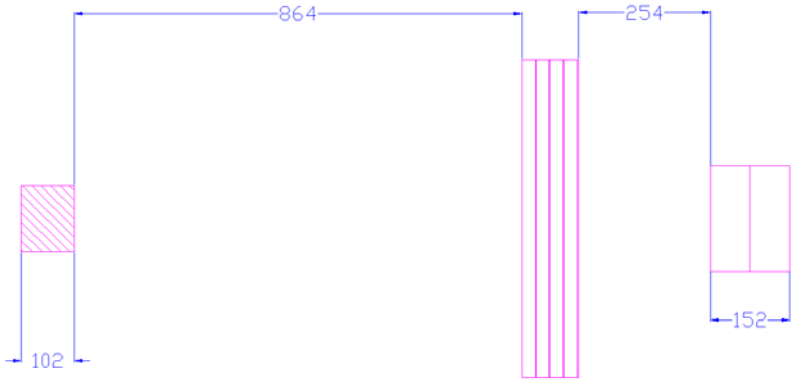

Figure 1. Schematic of target setup.

PENETRATION RESULTS

Table I lists the impact conditions, residual and eroded penetrator lengths, and normalized penetration into aluminum (target thickness normalized by eroded length, T/L_e) and steel (penetration normalized by residual length, P/L_{res}). Penetrators in all eight experiments impacted the targets with yaw values well below critical yaw. As Table I also shows, penetration into aluminum did not vary significantly for the velocities considered here. Further, these values are consistent with the penetration rate data obtained by Subramanian et al. [8].

TABLE I. TEST RESULTS

Shot #	Target Size (mm)	Rod D, mm	Velocity, (km/s)	Pitch (deg)	Yaw (deg)	Total Yaw α (deg)	Critical Yaw α_c (deg)	α/α_c	L_{res} (mm)	L_{eroded}, (mm)	Aluminum T/L_e	Steel P/L_{res}
820	100	6.35	2.14	0.9	-0.9	1.3	2.5	0.5	81.2	41.6	2.45	1.04
821	100	6.35	2.23	1.3	0.8	1.5	2.6	0.6	81.5	40.8	2.50	0.49
822	100	6.35	2.24	-0.4	-0.1	0.4	2.6	0.2	85.7	41.3	2.47	0.99
826	100	6.35	1.72	0.8	0.4	0.9	1.8	0.5	83.7	43.3	2.35	0.45
842	150	6.35	2.17	-1.1	-0.9	1.4	2.5	0.6	63.4	63.7	2.43	0.99
843	100	6.35	2.54	-0.5	1.1	1.2	3.2	0.4	85.6	41.4	2.46	1.13
844	150	6.35	1.76	0.6	-1.0	1.2	1.9	0.6	56.0	71.0	2.16	0.30
845	150	6.35	2.47	-0.3	0.3	0.4	3.1	0.1	62.7	64.3	2.41	1.15
871	100	9.53	2.15	-0.8	4.2	4.3	3.7	1.1	85.3	41.8	2.43	1.15
874	100	9.53	2.19	4.4	1.9	4.8	3.9	1.2	85.2	41.9	2.43	1.06
876	76	6.35	2.28	-0.4	1.5	1.6	2.7	0.6	95.9	31.1	2.45	1.28

Witness Plate Observations

After each experiment, the individual plates of the witness pack were backlit and photographed. This enabled the perforation pattern to be easily discerned. Figure 3 shows the plates from Shot 843. As seen, the number of holes decreases as the particles travel deeper into the array. These images were analyzed to obtain the total number of debris particles (from the number of holes in the witness plates), the hole positions, and the hole areas.

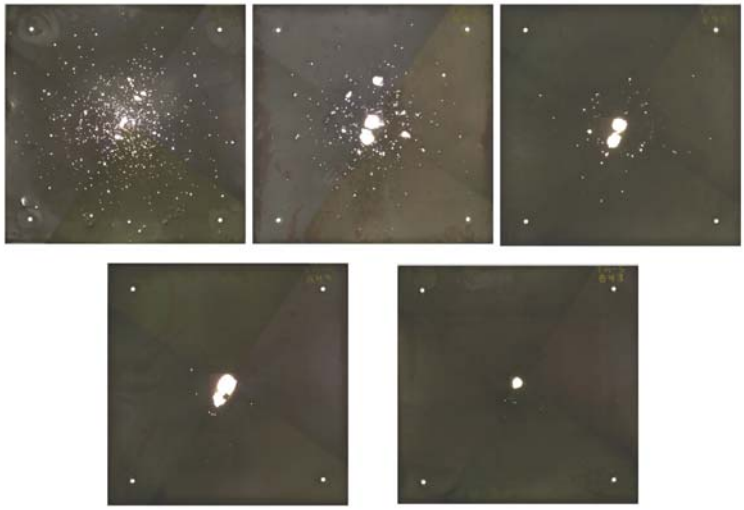

Figure 3. Sample witness plates from Shot 843.

Debris Cloud Characteristics

As previously mentioned, the witness plates were used to characterize the debris cloud. This technique gave the number of particles, their positions, and their hole areas. Figure 4 shows the effects of rod diameter, target thickness and velocity on the number of holes in the first witness plate.

As observed previously, as velocity increased, so too did the number of perforations in the first witness plate. This trend was found for the 100 and 150 mm thick targets. An increase in velocity of about 50% yielded a ~150% increase in the total number of debris particles generated.

The effect of target thickness on the debris was not the expected result. It was assumed that since thicker targets would erode more of the rod's length, more debris would be generated. However, despite a target thickness increase of 50% (between the 100 and 150 mm targets), the number of debris particles decreased for the 150 mm target for the three velocities considered. This was a surprising result given that the penetrators had about 37% (on average) more eroded length against the thicker target. The simplest explanation for the observation is that the debris that perforates the witness plates is primarily generated near the exit face of the target and not from the target interior. The trend was inconsistent as the thinnest target generated the fewest debris particles of all the tests around 2.2 km/s.

Finally, the effect of a 50% increase in rod diameter did not show an appreciable change in the total number of debris particles that perforated the first witness plate. However, as seen in Figure 5, the larger diameter rod did display an increase in the total number of holes in witness plates three through five. There are approximately twice as many "deep" holes for this rod as compared to the smaller diameter rod. This result implies that the particles had a greater penetrating power than those from the smaller

diameter rod. This agrees with the result from Farrand that showed the same trend for the low velocity tests he performed.

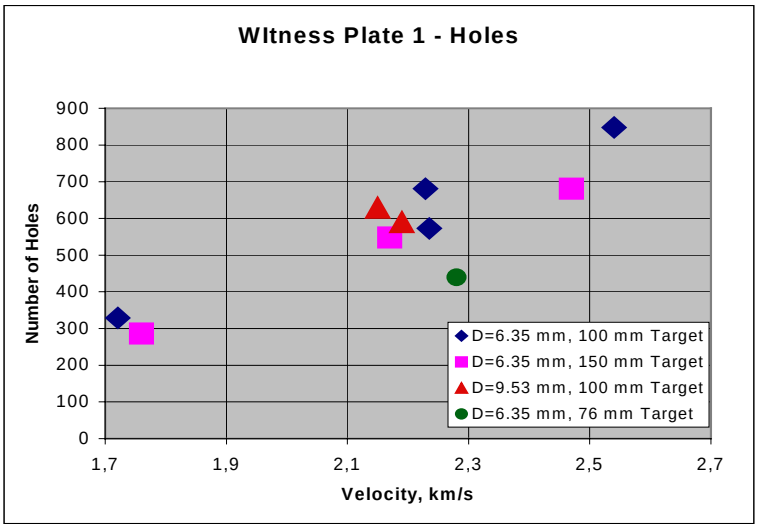

Figure 4. Number of holes in first witness plate.

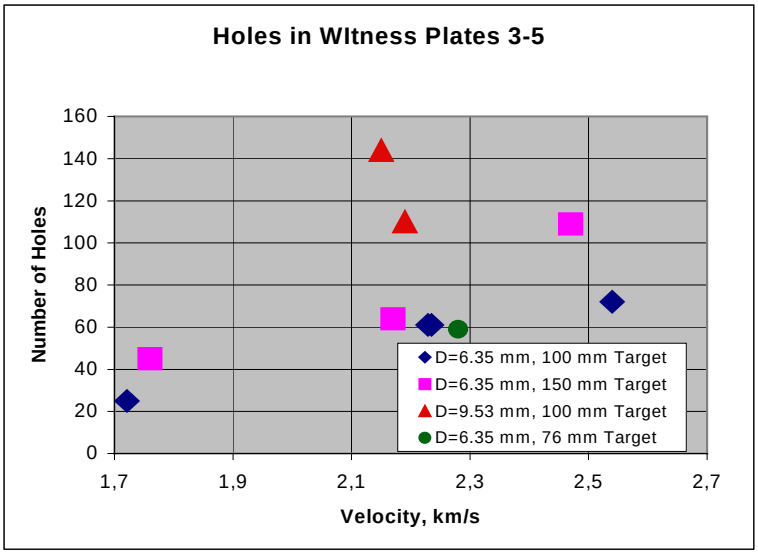

Figure 5. Total number of holes in witness plates three through five.

The larger diameter rod also generated debris particles that removed more total hole area from the first witness plates. The two tests with the larger rod removed the most area of all the tests at 2.2 km/s. This can be seen in Figure 6. One of the large diameter tests removed approximately the same area as the tests at 2.6 km/s despite having ~35% fewer holes created. Figure 7 shows the total area of the “deep” holes (the total area of

the holes in plates three through five). This also showed that the larger diameter rod had the greatest removed area of all tests.

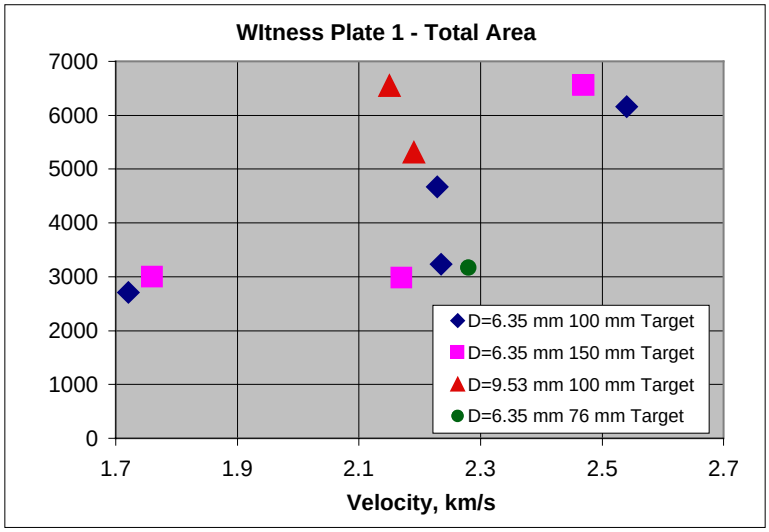

Figure 6. Total removed area from the first witness plate.

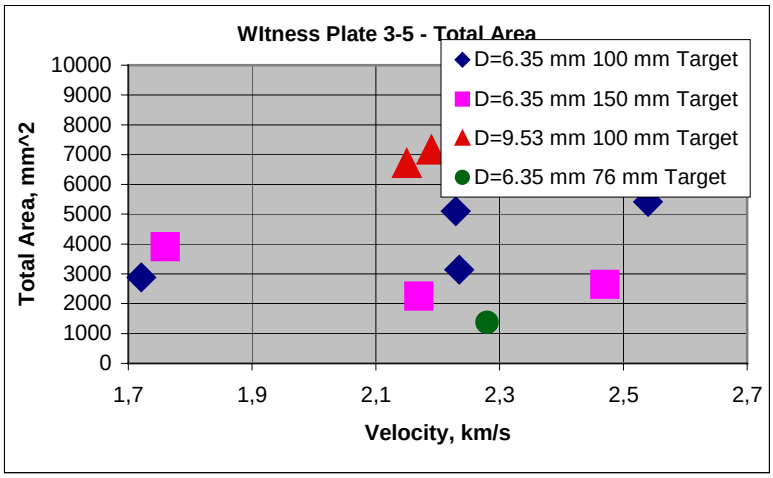

Figure 7. Total removed area from witness plates three through five.

The ratio of removed witness plate area for the larger and smaller diameter rods is A_2/A_1=1.48. This number, however, has a relatively large uncertainty. Taken together with the observation that the number of particles, N, does not change, bounds are placed on the dependence of particle size X (average particle dimension) and rod diameter, D.

If we assume equi-dimensional particles, and that they are generated over the eroded rod length, ΔL, then the total area of the generated particles can be estimated from the following.

$$N \propto \frac{D^2 \Delta L}{X^3}$$

$$X \propto \left(\frac{D^2 \Delta L}{N} \right)^{1/3}$$

$$A = NX^2 \propto N^{1/3} \Delta L^{2/3} D^{4/3}$$

From these equations, A_2/A_1 would be equal to 1.72 assuming that the number of particles and the eroded lengths are constant for the two rod diameters.

If we assume that the length of rod that contributes fragments to the debris is proportional to D, then

$$X \propto \frac{D}{N^{1/3}}$$

$$A \propto N^{1/3} D^2$$

From these equations, A_2/A_1 would be equal to 2.25 assuming that the number of particles is the same for both rod diameters.

Clearly, the first hypothesis is in better agreement with the data. Hence, at least approximately, the particle size scales as $D^{2/3}$. The strain rate is proportional to D^{-1} while 2/3 is much higher than typical strain rate exponents. Therefore, strain rate may not be a good way of predicting the size of generated particles. If *X* were controlled by intrinsic parameters such as grain size or shear band spacing, we would expect it to be independent of *D*, which is clearly not the case. The physical causes for the *X:D* relationship are left to be understood.

CONCLUSIONS

In this experimental investigation, the main goal was to characterize behind-armor debris from the impact of WHA penetrators against aluminum targets. It was discovered that, as the impact velocity increased, the total number of particles also increased. A ~50% increase in velocity yielded a ~150% increase in the number of particles. This type of improvement was seen for both target thicknesses. The number of particles did not increase with target thickness. Finally, larger diameter rods generated debris that penetrated more deeply into the witness pack and removed more total area from the plates as well.

ACKNOWLEDGMENT

The research reported in this document was performed in connection with Contract number DAAD17-01-D-0001 with the US Army Research Laboratory.

REFERENCES

1. B. Pedersen, S. Bless, "Behind-armor Debris from the Impact of Hypervelocity Tungsten Penetrators," *International Journal of Impact Engineering*, vol. 33 (2006), pp. 605-614.
2. B. Pedersen, S. Bless, "Characterization of Behind-armor Debris Particles from Tungsten Penetrators," 22nd International Symposium on Ballistics, Vancouver, BC, Canada, November 2005.
3. C. Anderson, S. Bless, T. Sharon, R. Subramanian, "Analysis of Behind Armor Debris at Two Impact Velocities," 15th International Symposium on Ballistics, Israel, May 1995.
4. C. Anderson, S. Bless, T. Sharon, R. Subramanian, "Behind Armor Debris Comparisons at Ordnance and Hypervelocity," TARDEC Combat Vehicle Survivability Symposium, March 28–30, 1995, Monterey, CA.
5. N. Lynch, "Constant Kinetic Energy Impacts of Scale Size KE Projectiles at Ordnance and Hypervelocity," *International Journal of Impact Engineering*, vol. 23 (1999), pp. 573–584.
6. V. Hohler, K. Kleinschitger, E. Schmolinske, A. Stilp, K. Weber, M, Mayseless, N. Sela, "Debris Cloud Expansion Around a Residual Rod Behind a Perforated Plate Target," 13th International Symposium on Ballistics, Stockholm, June 1992.
7. T. Farrand, J. Polesne, J. Abell, "Prediction of Behind Armor Debris Generated for Kinetic Energy Penetrators Against Light Armors," 16th International Symposium on Ballistics, San Francisco, CA, September, 1996.
8. R. Subramanian, S. Bless, J. Cazamias, D. Berry, "Reverse Impact Experiments Against Tungsten Rods and Results for Aluminum Penetration Between 1.5 and 4.2 km/s," *International Journal of Impact Engineering*, vol. 17 (1995), pp. 817–824.